This is a repository copy of *Evolution and progressive geomorphic manifestation of surface faulting: A comparison of the Wairau and Awatere faults, South Island, New Zealand*.

White Rose Research Online URL for this paper:
http://eprints.whiterose.ac.uk/108548/

Version: Accepted Version

Article:

Zinke_et_al_2015_Geology

Evolution and progressive geomorphic manifestation of surface faulting: A comparison of the Wairau and Awatere faults, South Island, New Zealand

Robert Zinke[1], James F. Dolan[1], Russell Van Dissen[2], Jessica R. Grenader[1], Edward J. Rhodes[3,4], Christopher P. McGuire[4],
Robert M. Langridge[2], Andy Nicol[5], and Alexandra E. Hatem[1]
[1]Department of Earth Sciences, University of Southern California, Los Angeles, California 90089, USA
[2]Institute of Geological and Nuclear Sciences, PO Box 30-368, Lower Hutt, New Zealand
[3]Department of Geography, University of Sheffield, Western Bank, Sheffield S10 2TN, UK
[4]Department of Earth, Planetary, and Space Sciences, University of California–Los Angeles, Los Angeles, California 90095, USA
[5]Department of Geological Sciences, University of Canterbury, Christchurch, New Zealand

ABSTRACT
Field mapping and lidar analysis of surface faulting patterns expressed in flights of geologically similar fluvial terraces at the wellknown Branch River and Saxton River sites along the Wairau (Alpine) and Awatere strike-slip faults, South Island, New Zealand, reveal that fault-related deformation patterns expressed in the topography at these sites are markedly less structurally complex along the higherdisplacement (hundreds of kilometers), structurally mature Wairau fault than along the Awatere fault (~13–20 km total slip). These differences, which are generally representative of the surface traces of these faults, provide direct evidence that surface faulting becomes structurally simpler with increasing cumulative fault offset. We also examine the degree to which off-fault deformation (OFD) is expressed in the landscape at the Saxton River site along the less structurally mature Awatere fault. Significantly greater amounts of OFD is discernible as a wide damage zone (~460 m fault-perpendicular width) in older (ca. 15 ka), more-displaced (64–74 m) fluvial terraces than in younger (ca. 1–7 ka), less-displaced (<55 m) terraces; no OFD is discernible in the lidar data on the least-displaced (<35 m) terraces. From this, we infer that OFD becomes progressively more geomorphically apparent with accumulating displacement. These observations imply that (1) the processes that accommodate OFD are active during each earthquake, but may not be evident in deposits that have experienced relatively small displacements; (2) structures accommodating OFD will become progressively geomorphically clearer with increasing displacement; (3) geomorphic measurements of overall fault zone width taken in deposits that have experienced small displacements will be underestimates; and (4) fault slip rates based on geomorphic surface offsets will be underestimates for immature faults if based solely on measurements along the high-strain fault core.

INTRODUCTION
As faults accumulate greater amounts of displacement, strain progressively localizes into a relatively narrow, structurally simple zone (e.g., Wesnousky, 1988; Chester et al., 2004; Dolan and Haravitch, 2014; Hatem, 2014). This process, known as structural maturation, decreases the proportion of total shear accommodated as off-fault deformation (OFD), which includes secondary faulting, warping, rotation, and distributed granular flow, that occur outside the fault core (e.g., Dolan and Haravitch, 2014). Additionally, the width and expression of OFD in geologic and geomorphic features will increase as deformation accumulates over multiple earthquakes, especially along structurally immature faults. In this way, the style and structural complexity of surface deformation recorded in recent deposits

along a fault will reflect both the structural maturity of the underlying fault as well as the cumulative deformation resulting from earthquakes experienced by the deposit. Understanding how these processes become manifest in the landscape is essential to the proper geomorphic interpretation of surface faulting patterns.

We examine the relationships between structural maturity, strain localization, and the geomorphic expression of OFD by characterizing surface faulting patterns along two strike-slip faults with vastly different cumulative displacements. Specifically, we combine field observations with aerial lidar topographic data to compare surface faulting patterns in flights of fluvial terraces at the Branch River and Saxton River sites along the Wairau and Awatere faults in the Marlborough fault system of South Island, New Zealand (Fig. 1). These observations provide key insights into the interplay between overall fault structural maturity and the progressive geomorphic manifestation of OFD with increasing fault offset in young deposits.

COMPARISON OF SURFACE DEFORMATION PATTERNS ALONG FAULTS WITH DIFFERENT STRUCTURAL MATURITIES

The Wairau and Awatere faults have similar slip rates, lithologies, and tectonic settings (see the GSA Data Repository1; e.g., Wallace et al., 2012, and references therein), but have accommodated considerably different amounts of slip. Whereas the Wairau fault has accommodated much of the total ~460 km of right-lateral offset along the Alpine fault system, the Awatere fault has accommodated only ~13–20 km of strike slip (Fig. 1; Fig. DR1 in the Data Repository; Sutherland, 1999; Rattenbury et al., 2006; this study). As a first-order observation, the Wairau fault is geomorphically and structurally simpler over its length than the Awatere fault (e.g., Fig. DR2; Rattenbury et al., 2006). Fault surface expressions are, however, subject to numerous variables, including variations in the age, composition, fabric, and thickness of the near-surface geologic material through which the fault propagates (e.g., Zinke et al., 2014b; Teran et al., 2015). The Branch River and Saxton River sites are ideal for comparing surface deformation patterns on these faults, as both consist of flights of fluvial terraces that are similar in depositional age, geologic material, grain size, fault slip experienced by the deposits, and climate. We adopt the names and interpretations of the terraces used by previous workers at each site (Fig. 2; Lensen, 1968; Mason et al., 2006). Seven terraces (A–F and W in Fig. 2A) compose the flight at Branch River, whereas the Saxton River site contains six terraces (T1–T6 in Fig. 2B) and a bedrock promontory ("bedrock spur" of Mason et al., 2006). The terrace deposits at both of these sites consist of greywacke-dominated cobble gravels. Luminescence dating and cobble weathering-rind analyses indicate that the terrace ages at Branch River (7–18 ka) overlap with those at Saxton River (0–15 ka) (Knuepfer, 1992; Mason et al., 2006). Moreover, the oldest terraces at each site have experienced similar amounts of displacement (53 ± 2 m at Branch River; 69 ± 5 m at Saxton River [see the Data Repository; Lensen, 1968; Mason et al., 2006; Grenader et al., 2014; Zinke et al., 2014a]).

We used high-resolution (≥12 shots m–2) aerial lidar topographic data (see details in the Data Repository) to map fault-related deformation expressed in the micro-topography (Fig. 2; Fig. DR3). Field observations of surface deformation at these sites support our lidar mapping. At both sites, subtle (≥20 cm) intra-terrace channels and geomorphically expressed minor secondary faults are well preserved in the landscape. Throughout both study sites, secondary faulting expressed by vertical relief on this order is the only form of OFD discernible in the lidar data, and in the following we use the distribution of secondary faults as a proxy for other, geomorphically undetectable forms of OFD (e.g., warping, distributed granular flow).

The trace of the Wairau fault at Branch River (Fig. 2A) is straight and continuous over most of the 1.2-km-long study area, though we note the presence of a sag basin and a pop-up ridge near the eastern edge of the study area, each expressed by 2–3 m of topographic

relief in terrace A. No secondary fault strands are geomorphically evident in the youngest four terraces (F–C). Two secondary fault strands, which are subparallel to the main trace, are discernible in the older W and A terraces. The faultper pendicular width of geomorphically evident deformation at this site is <100 m at its widest and is effectively discrete (<3 m wide) along ~80% of the length of the study site in all but the oldest, most-displaced terraces.

In contrast, the surface expression of the Awatere fault at Saxton River (Fig. 2B) is much more structurally complex. The main fault trace is multi-stranded throughout most of its length, and the main fault strands exhibit curvature on the half-kilometer scale. A 160-m-long, 2-m-deep sag basin is evident in the oldest T1 surface. The most striking difference in fault trace complexity between the two study sites is the abundance of secondary fault strands along the Awatere fault. These secondary faults are 14–342 m in length and are expressed by 0.2- to 1.1-m-tall scarps. Secondary fault strands are discernible to a maximum fault-perpendicular width of ~460 m in the oldest terrace, T1.

The Branch River and Saxton River sites are generally representative of surface deformation patterns along the Wairau and Awatere faults, as similar trends in structural complexity are observed along the entire 40 km and 80 km fault lengths covered by our lidar data (Fig. DR2). Although sections of relatively structurally simple surface faulting occur at some locations along the Awatere fault, such examples are not representative of the overall structural complexity of this structurally less-mature fault. We also note that the wider zone of OFD at Saxton River is not a function of thicker sediments at that site, as the terrace gravels are only a few meters thick there (Mason, 2004), whereas they are ≥10 m thick at the structurally simpler Branch River site (observed in nearby cut banks).

We suggest that the dearth of OFD expressed as secondary faulting at the Branch River site, relative to that at the Saxton River site, results from the greater cumulative offset and consequent higher structural maturity of the Wairau fault. This inference is consistent with previous theoretical and observational studies that demonstrate that whereas faulting may be complex and relatively diffuse along lower-displacement, structurally immature faults, strain progressively localizes into a relatively discrete, structurally simple zone with increasing amounts of displacement (e.g., Sibson, 1985; Wesnousky, 1988; Stirling et al., 1996; Frost et al., 2009; Dolan and Haravitch, 2014).

Changes in fault structure will lead to the co-evolution of many important fault behaviors. Structural complexities such as steps and bends exert strong controls on fault rupture arrest, so structurally simpler faults will tend to rupture in larger events (e.g., Wesnousky, 1988, 2006; Stirling et al., 1996; Elliott et al., 2009). Additionally, the frequency content of seismic energy released in earthquakes likely depends on fault complexity (Dolan, 2006). Furthermore, fault structural maturity exerts a primary control on percentages of OFD in large (M_W > 7) earthquakes (Dolan and Haravitch, 2014). Percentages of OFD can also affect measurements of slip in past earthquakes, with implications for the proper interpretation of fault slip rates based on offset geomorphic features and for the use of such data in seismic hazard assessments (Dolan and Haravitch, 2014).

PROGRESSIVE GEOMORPHIC MANIFESTATION OF OFD WITH INCREASING FAULT SLIP

The distribution of OFD expressed as secondary fault strands is strongly heterogeneous across the Saxton River site (Fig. 2B). In the oldest T1 surface, secondary faults discernible in the lidar define a zone of deformation across a total fault-perpendicular width of ~460 m. Secondary faults evident in the younger T2 surface define a narrower deformation zone with a fault-perpendicular width of ~100 m. OFD is also evident in the bedrock spur at fault-perpendicular distances of ~220 m north of the main fault trace (the same distance as OFD

in the adjacent T1 terrace) and ~30 m south of the main fault trace, though some evidence for OFD south of the main fault trace may be obscured by colluvium or destroyed by slumping. Regardless, the total width of OFD within the bedrock spur evident in the lidar is ≥230 m. In contrast to these wide zones of secondary faulting in the older deposits, no geomorphic evidence of OFD is visible in either the lidar data or in our field mapping in the T3–T6 surfaces. In these younger terraces, the fault is expressed as a single, discrete, through-going feature.

Given that flights of fluvial terraces such as those at Saxton River represent time-transgressive sequences of deposits, the observations above indicate that OFD becomes more geomorphically discernible in progressively older terraces. The lack of topographically expressed OFD in the T6–T3 terraces is not likely to reflect changes in the structural maturity of the bedrock Awatere fault beneath the terrace deposits, that occurred during the additional ~19 m of displacement accommodated between formation of the T2 and T3 terraces, as tens of kilometers of fault slip is necessary to cause such an increase in structural maturity (e.g., Wesnousky, 1988; Stirling et al., 1996; Dolan and Haravitch, 2014). Rather, the processes that accommodate OFD are equally active during each earthquake recorded at the Saxton River site. Variations in the thicknesses of the gravel deposits composing each terrace could influence the distribution of fault-related deformation, such that thicker gravel deposits would cause more OFD (e.g., Van Dissen et al., 2011; Zinke et al., 2014b; Teran et al., 2015). Paleoseismic trenching revealed bedrock as shallow as ~1.2 m below the T1 surface (Mason, 2004), whereas a road cut along the T2–T6 terrace riser exposes bedrock cropping out at 2–3 m below the T2 surface, suggesting that the T1 terrace gravels are similar in thickness to, or somewhat thinner than, the deposits composing the younger T2–T6 terraces. The fact that we observe more OFD in the T1 terrace than in the slightly thicker T2–T6 terraces reinforces our argument that cumulative slip, not sediment thickness, is the primary control on the manifestation of OFD in the landscape at Saxton River. Thus, whereas OFD may not be immediately evident in the landscape, it will become geomorphically better expressed as a function of increasing displacement (Fig. 3). In gravel dominated deposits such as those at Saxton River, along faults of similar structural maturity to the Awatere fault, 35–50 m of displacement may be necessary for OFD to become geomorphically evident.

We observe a similar though much less-pronounced relationship between OFD and terrace displacement on the Wairau fault at Branch River. Whereas no OFD is observable in the lidar along the five youngest, leastoffset terraces (F–B), we observe minor secondary faulting, out to ~90 m fault-perpendicular width, in the two oldest terraces (W and A) which have been displaced by ≥~55 m (Fig. 2). We reemphasize, however, that the dearth of geomorphically expressed OFD at the Branch River site relative to that at the Saxton River site in similarly offset terraces supports our inference that strain is much more localized along the structurally mature Wairau fault than along the much less-mature Awatere fault.

Analysis of surface deformation patterns associated with recent largemagnitude earthquakes using remote sensing techniques and field studies of offset linear cultural features reveals that surface ruptures are commonly surrounded by zones of OFD that extend as much as several hundred meters perpendicular to the fault (e.g., Rockwell et al., 2002; Van Dissen et al., 2013; Zinke et al., 2014b; Milliner et al., 2015). As much as ~50% of total coseismic surface displacement can be accommodated as OFD along structurally immature faults (Dolan and Haravitch, 2014), and numerous geologic studies report evidence for off-fault coseismic strain (e.g., cracking, en echelon shearing) associated with recent surface ruptures (e.g., Zinke et al., 2014b; Teran et al., 2015). Yet quantifiable evidence of OFD is seldom manifest in the surrounding geomorphology, as many of the structures that accommodate OFD during surface ruptures are not likely to be preserved in the landscape. Thus, despite the importance of OFD in accommodating coseismic surface strain, well-

defined geomorphic evidence for these zones that is likely to remain discernible for centuries to millennia is commonly lacking.

Geomorphic measurements of overall fault zone width may thus underestimate the true width of the fault zone, especially in deposits that have experienced small displacements along structurally immature faults. The ability to predict the width of fault-related deformation in advance of future events is important for understanding fault rupture mechanics and mitigation of seismic hazards to the built environment. For instance, improved constraints on expected surface deformation patterns could aid in the potential development of earthquake hazard microzonation maps detailing the expected magnitude and width of OFD, which in turn could be incorporated into design standards for more effective earthquake-resistant design. Furthermore, failure to account for OFD in geomorphic measurements of fault slip may lead to systematic underestimation of the total fault slip, and consequently to underestimation of paleoearthquake magnitudes and fault slip rates. Because fault slip rates are a basic input into most probabilistic seismic hazard analyses, this will lead to underestimation of the seismic hazard associated with a fault. Proper interpretation of fault-related deformation patterns in the landscape therefore rests on the recognition that although OFD may not be fully geomorphically expressed, the processes that accommodate OFD nevertheless play a crucial role in accommodating coseismic strain in the near surface, especially along structurally immature faults.

REFERENCES CITED

Chester, F. M., Chester, J. S., Kirschner, D. L., Schulz, S. E., and Evans, J. P., 2004, Structure of large-displacement, strike-slip fault zones in the brittle continental crust, in Karner, G.D., et al., eds., Rheology and Deformation of the Lithosphere at Continental Margins: New York, Columbia University Press, p. 223–260.
DeMets, C., Gordon, R.G., Argus, D.F., and Stein, S., 1994, Effect of recent revisions to the geomagnetic reversal time scale on estimates of current plate motions: Geophysical Research Letters, v. 21, p. 2191–2194, doi: 10.1029 /94GL02118.
Dolan, J.F., 2006, Seismology: Greatness thrust upon them: Nature, v. 444, p. 276–279, doi:10.1038/444276a.
Dolan, J.F., and Haravitch, B., 2014, How well do surface slip measurements track slip at depth in large strike-slip earthquakes? The importance of fault structural maturity in controlling on-fault slip versus off-fault surface deformation: Earth and Planetary Science Letters, v. 388, p. 38–47, doi:10.1016/j .epsl .2013 .11.043.
Elliott, A.J., Dolan, J.F., and Oglesby, D.D., 2009, Evidence from coseismic slip gradients for dynamic control on rupture propagation and arrest through stepovers: Journal of Geophysical Research, v. 114, B02312, doi: 10.1029 /2008jb005969.
Frost, E., Dolan, J.F., Sammis, C., Hacker, B., Cole, J., and Ratschbacher, L., 2009, Progressive strain localization in a major strike-slip fault exhumed from midseismogenic depths: Structural observations from the Salzach- Ennestal-Mariazell-Puchberg fault system, Austria: Journal of Geophysical Research, v. 114, B04406, doi:10.1029/2008jb005763.
Grenader, J., Dolan, J.F., Rhodes, E.J., Van Dissen, R.J., Langridge, R., Zinke, R.W., McGuire, C.P., and Nicol, A., 2014, Analysis of a new Marlborough Fault System lidar

dataset: The Wairau and Hope faults, South Island, New Zealand: Eos (Transactions, American Geophysical Union), v. 95, abstract T41C4653.

Hatem, A.E., 2014, Evolution of off-fault deformation along analog strike-slip faults [M.S. thesis]: Amherst, University of Massachusetts, Paper 90, 90 p.

Knuepfer, P.L.K., 1992, Temporal variations in latest Quaternary slip across the Australian-Pacific plate boundary, northeastern South Island, New-Zealand: Tectonics, v. 11, p. 449–464, doi:10.1029/91TC02890.

Lensen, G.J., 1968, Analysis of progressive fault displacement during downcutting at the Branch River terraces, South Island, New Zealand: Geological Society of America Bulletin, v. 79, p. 545–556, doi:10.1130/0016 -7606 (1968) 79 [545 :AOPFDD]2.0 .CO;2.

Mason, D.P.M., 2004, Neotectonics and paleoseismicity of a major junction between two strands of the Awatere Fault, South Island, New Zealand [M.S. thesis]: Wellington, New Zealand, Victoria University of Wellington, 173 p.

Mason, D.P.M., Little, T.A., and Van Dissen, R.J., 2006, Rates of active faulting during late Quaternary fluvial terrace formation at Saxton River, Awatere fault, New Zealand: Geological Society of America Bulletin, v. 118, p. 1431–1446, doi:10.1130/B25961.1.

Milliner, C.W.D., Dolan, J.F., Hollingsworth, J., Leprince, S., Ayoub, F., and Sammis, C.G., 2015, Quantifying near-field and off-fault deformation patterns of the 1992 MW 7.3 Landers earthquake: Geochemistry Geophysics Geosystems, v. 16, p. 1577–1598, doi:10.1002/2014GC005693.

Rattenbury, M.S., Townsend, D.B., and Johnston, M.R., compilers, 2006, Geology of the Kaikoura area: New Zealand Institute of Geological & Nuclear Sciences 1:250 000 Geological Map 13, scale 1:250,000, 1 sheet, 70 p. text.

Rockwell, T.K., Lindvall, S., Dawson, T., Langridge, R., Lettis, W., and Klinger, Y., 2002, Lateral offsets on surveyed cultural features resulting from the 1999 Izmit and Duzce earthquakes, Turkey: Bulletin of the Seismological Society of America, v. 92, p. 79–94, doi:10.1785/0120000809.

Sibson, R.H., 1985, Stopping of earthquake ruptures at dilational fault jogs: Nature, v. 316, p. 248–251, doi:10.1038/316248a0.

Stirling, M.W., Wesnousky, S.G., and Shimazaki, K., 1996, Fault trace complexity, cumulative slip, and the shape of the magnitude-frequency distribution for strike-slip faults: A global survey: Geophysical Journal International, v. 124, p. 833–868, doi:10.1111/j.1365-246X.1996.tb05641.x.

Sutherland, R., 1999, Cenozoic bending of New Zealand basement terranes and Alpine Fault displacement: A brief review: New Zealand Journal of Geology and Geophysics, v. 42, p. 295–301, doi:10.1080/00288306.1999.9514846.

Teran, O.J., Fletcher, J.M., Oskin, M.E., Rockwell, T.K., Hudnut, K.W., Spelz, R.M., Akciz, S.O., Hernandez-Flores, A.P., and Morelan, A.E., 2015, Geologic and structural controls on rupture zone fabric: A field-based study of the 2010 MW 7.2 El Mayor–Cucapah earthquake surface rupture: Geosphere, v. 11, p. 899–920, doi:10.1130/GES01078.1.

Van Dissen, R., et al., 2011, Surface rupture displacement on the Greendale Fault during the MW 7.1 Darfield (Canterbury) earthquake, New Zealand, and its impact on man-made structures, in Proceedings of the Ninth Pacific Conference on Earthquake Engineering: Building an Earthquake-Resilient Society, Auckland, New Zealand, 14–16 April: Wellington, New Zealand, New Zealand Society for Earthquake Engineering Paper 186, 8 p.

Van Dissen, R., Hornblow, S., Quigley, M., Litchfield, N., Villamor, P., Nicol, A., Barrell, D.J.A., Sasnett, P., and Newton, K., 2013, Towards the development of design curves for characterising distributed strike-slip surface fault rupture displacement: An example from the 4 September, 2010, Greendale Fault rupture, New Zealand, in Chin, C.Y., ed., Proceedings of the 19th NZGS (New Zealand Geotechnical Society) Geotechnical Symposium, Queenstown, New Zealand, 20–23 November: Wellington, New Zealand, New Zealand Geotechnical Society, p. 455–462.

Wallace, L.M., Barnes, P., Beavan, J., Van Dissen, R., Litchfield, N., Mountjoy, J., Langridge, R., Lamarche, G., and Pondard, N., 2012, The kinematics of a transition from

subduction to strike-slip: An example from the central New Zealand plate boundary: Journal of Geophysical Research, v. 117, B02405, doi: 10.1029 /2011jb008640.

Wesnousky, S.G., 1988, Seismological and structural evolution of strike-slip faults: Nature, v. 335, p. 340–343, doi:10.1038/335340a0.

Wesnousky, S.G., 2006, Predicting the endpoints of earthquake ruptures: Nature, v. 444, p. 358–360, doi:10.1038/nature05275.

Zinke, R., Dolan, J.F., Rhodes, E.J., Van Dissen, R., Langridge, R., Grenader, J., McGuire, C.P., and Nicol, A., 2014a, Analysis of high-resolution lidar digital topographic data along the Marlborough Fault System: The Awatere and Clarence faults, South Island, New Zealand: Eos (Transactions, American Geophysical Union), v. 95, abstract T41C-4652.

Zinke, R., Hollingsworth, J., and Dolan, J.F., 2014b, Surface slip and off-fault deformation patterns in the 2013 MW 7.7 Balochistan, Pakistan earthquake: Implications for controls on the distribution of near-surface coseismic slip: Geochemistry Geophysics Geosystems, v. 15, p. 5034–5050, doi: 10.1002/2014GC005538.
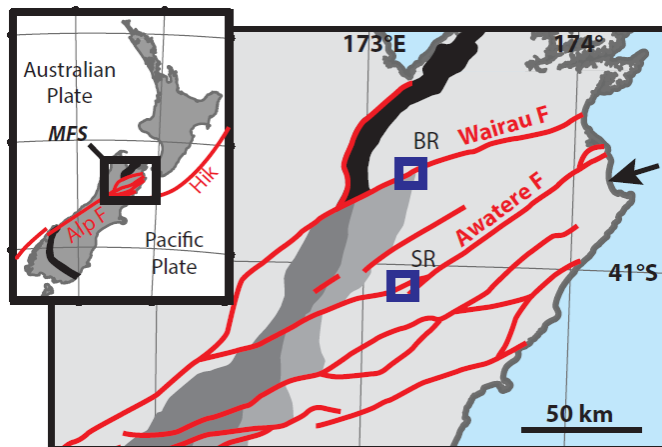
Figure 1. Inset: Marlborough fault system (MFS) on South Island, New Zealand, transfers relative Pacific-Australian plate motion between dextral-oblique–slip Alpine fault (Alp F) and Hikurangi subduction margin (Hik). Wairau fault has accommodated much of the ~460 km of right-lateral shear along the Alpine fault system, as shown by Dun Mountain–Maitai ultramafic terrane (black) (Sutherland, 1999). Main figure: Simplified representation of MFS showing active, predominantly strike-slip faults in red. Black arrow shows Pacific plate motion relative to Australian plate (DeMets et al., 1994). Rakaia (dark gray) and Esk Head (medium gray) basement terranes are offset ~13 km along Awatere fault by discrete slip, with potential additional ~5 km of slip manifest as bending ("drag folding") of terrane boundaries (Rattenbury et al., 2006). Branch River (BR) and Saxton River (SR) sites are shown.
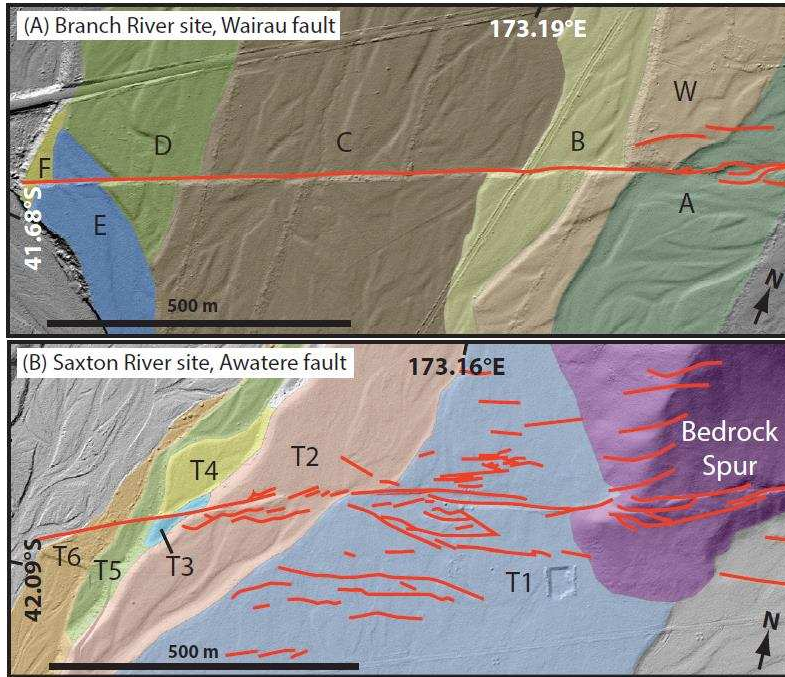
Figure 2. Lidar hillshade images of the two study sites in New Zealand. A: Branch River site on Wairau fault. B: Saxton River site on Awatere fault. Fault traces (including secondary fault strands) shown in red. Terraces are demarked by colours and labeled according to previous studies (Lensen, 1968; Mason et al., 2006). Contacts between coloured surfaces represent terrace risers.
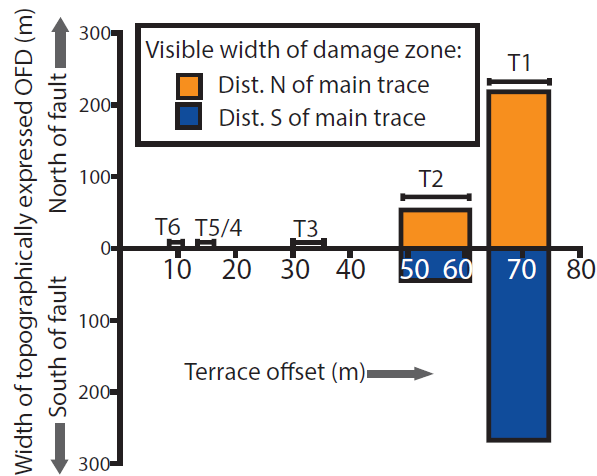

Figure 3. Fault-perpendicular width of geomorphically evident deformation at Saxton River (Awatere fault), New Zealand, as function of terrace offset. Terraces (T1–T6) are as shown in Fig. 2B. Width of boxes represents uncertainty in lateral terrace offset (Zinke et al., 2014a). Whereas strain per event accommodated as off-fault deformation (OFD) remains constant, secondary faults become better expressed as terraces accumulate slip. Dist.—distance.